

The PRESPEC liquid-hydrogen target for in-beam gamma spectroscopy of exotic nuclei at GSI

C. Louchart^a, J.M. Gheller^a, Ph. Chesny^a, G. Authelet^a, J.Y. Rousse^a,
A. Obertelli^a, P. Boutachkov^b, S. Pietri^b, F. Ameil^b, L. Audirac^a, A. Corsi^a,
Z. Dombradi^c, J. Gerl^b, A. Gillibert^a, W. Korten^a, E. Merchan^b, C.
Nociforo^b, D. Ralet^b, M. Reese^d, V. Stepanov^a

^aCEA, Centre de Saclay, IRFU, F-91191 Gif-sur-Yvette, France

^bGSI, D-64291 Darmstadt, Germany

^cATOMKI, P.O. Box 51, H-4001 Debrecen, Hungary

^dIKP, TU Darmstadt, D-64289 Darmstadt, Germany

Abstract

We report on a new liquid hydrogen target dedicated to in-beam gamma spectroscopy experiments in inverse kinematics at relativistic incident energies at GSI/FAIR. The target-cell and entrance window are composed of 200- μm thick Mylar. Target thicknesses from 10 to 60-mm can be reached for an effective diameter of 70 mm. The proposed design has the advantage of being free of absorbing material at forward angles and 90 degrees, allowing the detection of photons on a wide angular range. A commissioning experiment with a ^{54}Cr beam at 130 MeV/nucleon has been performed at GSI with the RISING setup. The target has been shown to behave as expected and is ready for experimental campaigns with AGATA.

Keywords:

1. Introduction

2 Exotic nuclei exhibit structure features that are different than those ob-
3 served in stable nuclei, such as clustering at low excitation energy or a modi-
4 fied single-particle shell structure. The development of dedicated radioactive-
5 beam facilities allows the study of these new phenomena. Unstable nuclei are
6 produced either at relativistic energies by fragmentation as in RIBF, RIKEN,
7 and GSI or by the Isotopic Separation On Line (ISOL) technique as at SPI-
8 RAL, GANIL, or ISOLDE, CERN. Beam intensities available for the most

9 exotic species are typically 10^4 pps down to less than a particle per second.
10 To counter-balance low beam intensities, the use of thick targets, when possi-
11 ble, is a straightforward way of increasing the luminosity. In this context,
12 in-beam gamma spectroscopy at relativistic energies in inverse kinematics
13 has been shown to be a powerful tool for the investigation of nuclear struc-
14 ture away from stability. Indeed, the combination of intermediate energies
15 and detection of gamma rays allow the use of very thick targets, with the
16 only restriction of reaching a sufficient energy resolution after Doppler-effect
17 reconstruction. The in-flight-emitted gamma ray measurement requires the
18 knowledge of the recoil velocity and the gamma emission angle to correct
19 the Doppler effect and access to the gamma energy in the rest frame of the
20 emitting nucleus. The efficiency of this correction relies on the accuracy with
21 which we determine these two quantities. The former depends on the gran-
22 ularity of γ ray detectors (size of Ge crystal) while the first is linked to the
23 interaction point in the target. The use of a thick target increases the un-
24 certainty on the interaction point position and therefore degrades the energy
25 resolution.

26 Several reaction mechanisms and target combinations can be used at rela-
27 tivistic energies to discover the properties of unstable nuclei. Most commonly
28 used, coulomb excitation and heavy-ion induced inelastic scattering exper-
29 iments allow to investigate the collectivity of nuclei, whereas one nucleon
30 knockout reactions have been used to populate single-particle states and test
31 structure model wave functions through the comparison of experimental and
32 theoretical cross sections. Among all possible material for the target, hy-
33 drogen offers unique advantages. It brings the possibility of using different
34 reaction mechanisms with a unique selectivity: proton inelastic scattering
35 (p,p') is sensitive to the neutron and proton collectivity, complementary to
36 coulomb excitation, and proton-induced knockout reactions such as (p,2p)
37 and (p,pn) are known to be the cleanest hadronic probe for spectroscopic
38 factor extraction from knockout reactions. An additional benefit of hydrogen
39 targets is the large number of scattering centers for a same energy loss in the
40 target compared to larger-atomic-number targets, such as ^9Be or ^{12}C . By us-
41 ing an hydrogen target for in-beam gamma spectroscopy, the luminosity can
42 be improved while containing the energy resolution. Another advantage of
43 pure hydrogen targets is the background reduction. The breakup of heavy-
44 ion targets may lead to the emission of neutrons and provoke background
45 events in the measured gamma spectra. Furthermore, less bremsstrahlung
46 contamination is expected when using a pure-hydrogen target compared to

47 heaviest-ion targets [?]. Consequently, a minimized signal over noise ratio
48 in the measured gamma spectra can be expected.

49

50 For these reasons, liquid or solid hydrogen targets have been developed to
51 study the nuclear structure all over the world, for instance at GANIL [?] and
52 RIKEN [?], the available thickness ranging from few millimeters to several
53 centimeters. A recent review of those different targets and applications could
54 be found in reference [?]. In this context, a thick liquid hydrogen target has
55 been developed by the cryogenic division of CEA. It is primarily dedicated to
56 experiments with the AGATA [?] demonstrator at GSI and, in the future,
57 to HISPEC campaigns with AGATA at FAIR.

58 In the following, the design of the target will be detailed in section 2 and
59 operating modes will be described in section 3. In the design of the present
60 target, particular attention has been focused on safety aspects which are sum-
61 marized in section ???. Results from a dedicated commissioning experiment
62 at GSI are finally presented in section ???.

63 2. Target design

64 The Magnetism and Cryogenics laboratory (SACM) of CEA-IRFU has
65 developed expertise in cryogenic targets including liquid and solid hydrogen
66 targets. Several targets have been designed for experiments at the Saturne
67 Laboratory, Saclay, from 1985 to 1997 and since 1998 for the Jefferson Labo-
68 ratory (targets for the POLDER and CLASS experiments), for the spallation
69 program at GSI (FRS1, FRS2 and SPALADIN targets [?]) and, more
70 recently, for upcoming low-energy experiments with radioactive beams at
71 SPIRAL2 [?]. The present liquid target is based on the use of a cryocooler,
72 limiting the amount of hydrogen in the liquefied active volume, enhancing
73 the safety related to the use of hydrogen. Particular attention is applied to
74 the target container itself, made of Mylar, whose thickness satisfies an accept-
75 able compromise between mechanical strength and transparency.

76

77 2.1. Overview

78 The installation is composed of two distinct parts (see Fig.1): the target
79 and the control of the system. They can be separate up to 15 meters. The the
80 target and its cryostat are installed in the experimental area. A cryocooler
81 (cold head and compressor) is used to reach temperature of about 20 K.

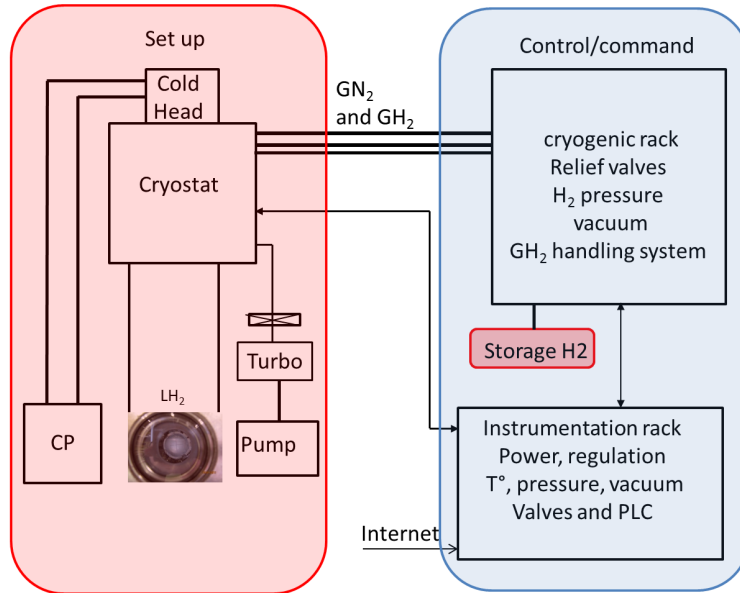


Figure 1: Synoptic of the system including (left) the target and cryostat and (right) the control-command.

82 The pumping system (turbo pump and primary pump) is located around the
 83 cryostat. A remote controle command is used to pilot all the installation and
 84 placed on the roof of the experimental room. It is composed of two racks:
 85 one is dedicated to cryogenics and the second to control temperature and
 86 pressure probes and valves. The gaseous hydrogen (GH₂) storage is connected
 87 to the cryogenic rack and the target. Different informations (vacuum, H₂
 88 pressure or cryocooling) can be viewed via a computer interface. A dedicated
 89 Programmable Logic Controller (PLC) controls the system.

90 2.2. The target cell

91 The target cell is made of two components: (i) a Mylar entrance window
 92 (125 μm thick and 6 cm in diameter) is glued on a stainless steel body
 93 (with filling and return gas tubes) (see the right picture of Fig.); (ii)
 94 Mylar exit window (150 μm thickness and 7.5 cm in diameter) forms the
 95 body of the target (see the left and middle pictures of Fig.). The cap were
 96 thermoformed at 160° by mechanical stamping. The two parts are gathered
 97 with an Helicoflex[®] seal. Elastic properties over a large range of temperature

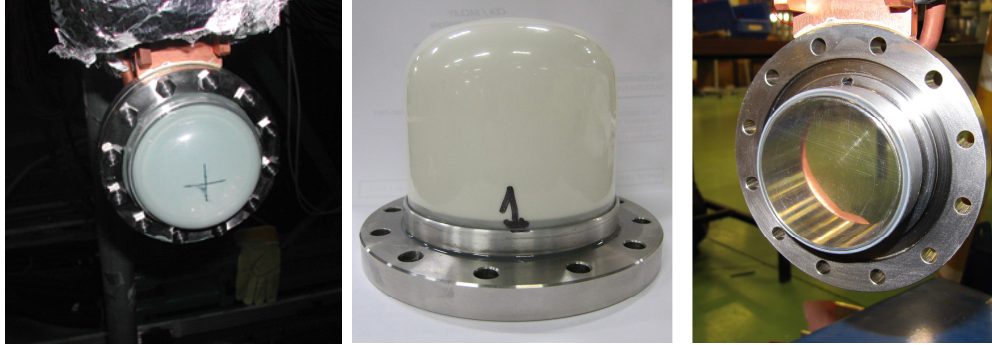


Figure 2: Target cell of the 20-mm thick target (left) and 20-mm target (middle). (Right) Entrance window of the target mounted on its flange.

98 of this Helicoflex[®] seal made of metal coated with aluminium ensured the
99 impermeability of the cell.

100

101 These Mylar envelopes are built with a dedicated set of tools designed to
102 obtain the desired geometry. The glue used is unique to withstand low tem-
103 peratures ($T \approx 77\text{ K}$) and remain flexible to overcome the differential shrinkage
104 of the materials used at 20 K (Mylar, aluminium and stainless steel). The
105 function of the glue is to ensure sealing between the different parts of the
106 target. To strengthen pasting needed by the internal pressure efforts (max-
107 imum internal pressure is 1330 mbar absolute at room temperature), two
108 aluminium rings are placed around the envelope of Mylar on the part of
109 stainless steel. These rings help (by contracting at low temperature) the
110 continuation of pasting. The Safety Manual of Fermi lab (ref?) recommends
111 a burst pressure for Mylar flask of at least 2.8 bars (internal differential pres-
112 sure). Results of three crash tests of the window and the container in Mylar
113 are 9,3 bars for entrance window and 11,3 bars for the container, well above
114 the widespread Fermi Lab safety rules.

115

116 *2.3. The cryostat*

117 The cryostat is mounted at the vertical of the target (see Fig. 3) on a
118 support, designed in agreement with the experimental environment. For the
119 commissioning experiment, the thermometry and the hydrogen and nitrogen
120 connections of the circuits are on the top of the cryostat at 3,50 meters high
121 above the ground. The compressor and the vacuum system were located on
122 the floor. The cryocooler is composed of two flexible loaded with helium gas,
123 connected between the compressor and cold head.

124 The cold head is on the top of the cryostat. Inside the cryostat (see Fig.3),
125 the thermally insulated from the exterior is a copper shield cooled by contact
126 with the first stage at 50 K. The condenser is mounted on the second stage
127 of the cold head. It is a copper cylinder 8.7 cm long and 14.1 cm in diameter.
128 Hydrogen is cooled and liquefied by contact inside it at 20.4 K. Liquid hy-
129 drogen formed flows by gravity to the target located in the lower part of the
130 cryostat. The target is fixed by a support at the bottom of the condenser.
131 The assembly is at liquid hydrogen temperature. The cold vapors contained
132 in the return tube of the target liquefy again in the condenser (the coldest
133 part of the cryogenic system). Then the liquid falls in the supply pipe of the
134 target which remains full. By the principle of thermo siphon, the target is
135 always supplied with liquid hydrogen.

136 *2.4. Control and command*

137 Piloting operations are conducted in the control command area. Cryo-
138 genic and instrumentations racks are connected together and to the cryostat.
139 The cryogenic rack permits to introduce hydrogen (or deuterium) gas from
140 the storage vessels to the target and also different processes like air emptying
141 of the H₂ circuit or vacuum chamber and the filling with N₂ gas. There are
142 manual valves, relief valves connected to discharge circuit, different manome-
143 ters, two pressure sensors and one primary vacuum gauge. A fully automatic
144 system piloted by the instrumentation rack permits the gas liquefaction. A
145 drive flow indicates the amount of hydrogen that is liquefied in the cryostat.

146
147 The instrumentation rack supplies electrical power (low and high voltage).
148 Several indicators give different informations : pressure, temperature, gas
149 flow, vacuum of the cryostat and the H₂ circuit. Automaton inputs/outputs
150 are connected to the different instruments of this installation (compressor,
151 pumps and a few valves) and all the informations given by the indicators.

152

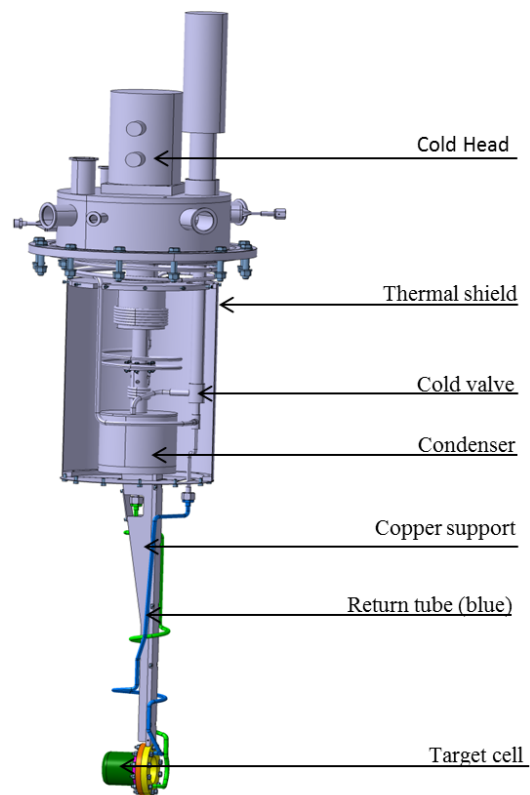


Figure 3: Global view of the cryostat and the target cell (in green).

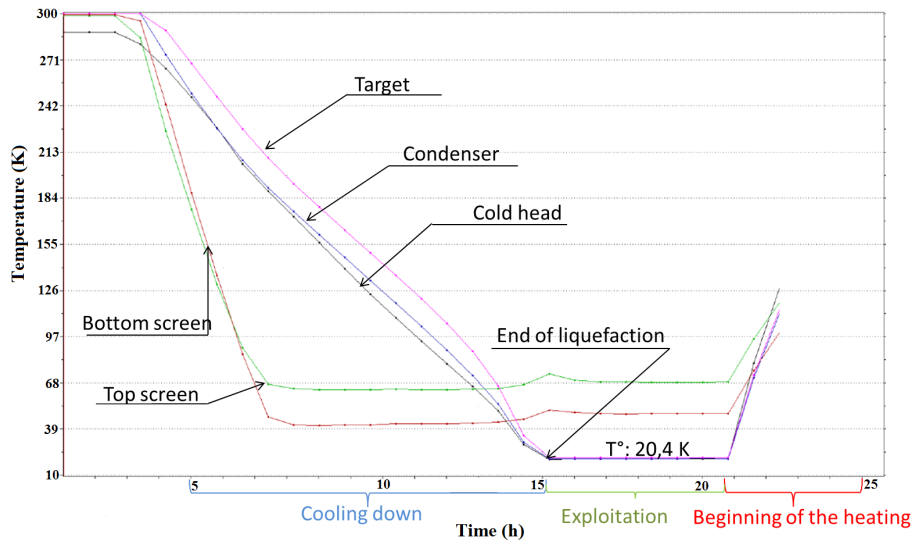


Figure 4: End of liquefaction

153 3. Operation modes

154 The installation has three working modes. Liquefaction mode during the
 155 cooling down and filling, Exploitation mode when the target is used for ex-
 156 periments and Stop Experiment mode during the target reheating and the
 157 gas return in the storage and the most important the securing of the cryostat
 158 by introducing N2 gas at the end.

159

160 3.1. Cooling

161 Liquefaction system is totally independent of the automaton. The gas
 162 flow is controlled by a proportional valve. The pressure set point during
 163 cooling down and liquefaction is adjusted to 1050 mbar (ABS). At the end of
 164 liquefaction, pressure transmitter of the H2 storage is adjusted to 1100 mbar
 165 (ABS). At this value, electro valve closes automatically (see Fig.4). After
 166 liquefaction a transient phase is inevitable during the pressure stabilisation.
 167 To avoid a liquefaction mode return, (gas returns through two relief valves
 168 to the storage) it will be necessary to close the electro valve.

169

170 *3.2. Running*

171 The automaton manages alarms by using the different set points neces-
172 sary to secure a normal working. Most alarms are only indicative and without
173 interaction with the operation. A few alarms activate automatic actions.

174

175 Note that the design of the system allows to empty the target in few
176 minuts, often mandatory for background measurement and subtraction to
177 the data. The closing of the cold valve stops the thermo siphon process and
178 the liquid hold in the target comes back and stays in the condenser because
179 the pressure is higher than the condenser (3 to 5 mbar). The empty target is
180 only filled with cold hydrogen vapor, i.e. of negligeable thickness compared
181 to the entrance and exit windows.

182

183 *3.3. Warming up*

184 **4. Safety considerations**

185 Hydrogen is cooled and liquefied by contact with the second stage of
186 the cold head. This configuration limits liquid volume to about 100 cm³.
187 The target and the refrigeration system are in an extra 100 litres vacuum
188 chamber which provides a secondary containment volume in case of a target
189 rupture. The target is connected to a 255 litres storage tank through two sep-
190 arate check valves. The exhaust from these valves will be evacuated outside
191 through the safety exhaust line. The final pressure in the storage tank will
192 be 1.05 bars (ABS). This eliminates any risk of explosion fuelled by oxygen
193 leaking into the system. Filling the target with hydrogen requires about 84
194 litres of gas NTP. As a result, the initial pressure of the storage tank is 1.33
195 bars before the hydrogen liquefaction. The total amount of hydrogen used
196 in the entire system is 340 litres of gas NTP. According to the Fermi lab
197 regulations, storage and use of flammable gases at physics experiments, our
198 system is classified as risk class 0 (hydrogen volume 7.4 m³). This still does
199 present some risk of potential explosion, so the system has been designed to
200 be fail-safe and constitutes a totally closed loop with two levels of contain-
201 ment.

202

203 The basic idea behind the handling of any flammable or explosive gas is
204 to remove oxygen and prevent exposure to an energy source that could cause
205 ignition. The source of oxygen in the atmosphere and ignition sources are

206 electrical equipment. The following general guidelines are used for designing
207 the gas handling system :

- 208 • no valves can open the system to air,
- 209 • each pressure monitor is spark-proof,
- 210 • the pumps used in the storage tank circuitry are leak-proof (hermetic).

211

212 *4.1. Handling of emergencies*

213 In the case of a compressed air failure and/or electrical failure, the target
214 is always connected to the storage tank via two relief valves (see Fig.??).
215 The final pressure in the target is the initial pressure in the tank. Protection
216 against blockage due to the solidification of a contaminating gas, such as
217 air, in the H₂ refrigeration circuit (no matter where the blockage occurs) is
218 ensured since the entrance and return target lines are connected to pressure
219 safety valves. During the transfer operation, the target condenser and cell
220 are protected against blockage by the radiation shield which pre-cools the gas
221 to 40 K; all gases other than hydrogen will be trapped there.

222 The target temperature is regulated by automaton. In case of a regulation
223 system loss there is a risk of a hydrogen solidification which could lead to
224 target damaging. To avoid such a problem, the compressor is automati-
225 cally stopped when the target pressure reaches a threshold value of 310 mbar
226 (equivalent temperature 17K) which is given directly by the pressure trans-
227 mitter.

228

229 *4.2. Loss of vacuum in the chamber*

230 Loss of vacuum in the chamber represents the highest level of emergency
231 in the system because of potential hydrogen leak. The following actions are
232 automatically realized:

- 233 • vacuum pump is stopped during cooling down phase,
- 234 • compressor is stopped,
- 235 • verify that manual valves are closed (normal status) to avoid addi-
236 tional hydrogen coming from the storage tank. The gas will go back to
237 the storage tank via pressure safety valves.

238

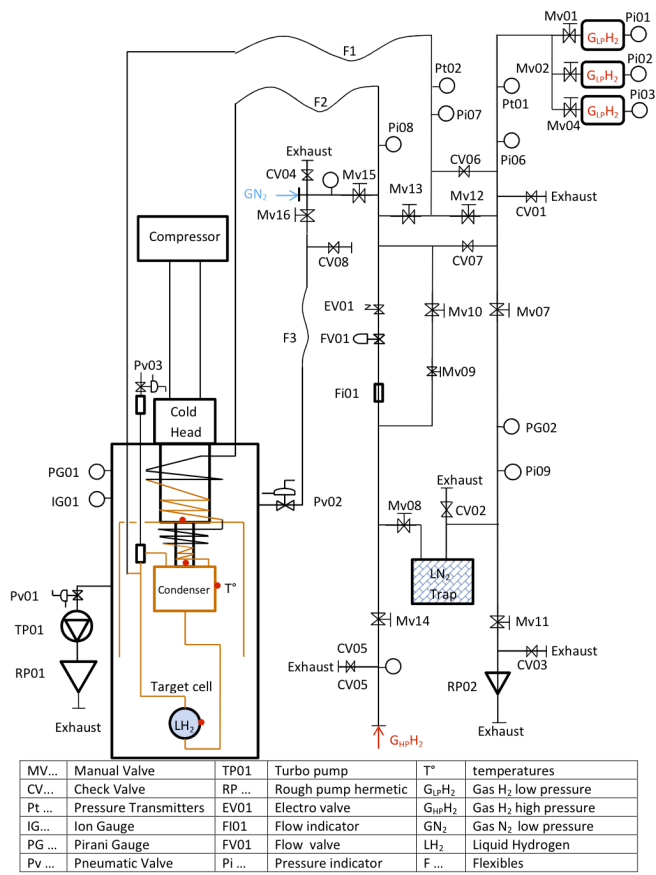


Figure 5: the schematic diagram of the hydrogen circuitry.

239 *4.3. Rupture of the target cell*

240 First of all, there is a deposition of the flask contents into the vacuum
241 space. The maximum pressure in the vacuum chamber and the storage tank
242 will be respectively 0.84 bars and 1.05 bars. The residual gas in the vacuum
243 chamber has to be evacuated manually with pump. (?)

244 In the case, very unlikely, of a simultaneously closing of storage tank man-
245 ual valves and a target cell rupture, the maximum pressure in the vacuum
246 chamber is always 0.84 bars. In any case, there is no need for check valves on
247 the vacuum chamber to evacuate the gas as the final pressure is low enough.
248 There is no risk to have a vacuum chamber failure.

249

250 **5. Commissioning experiment**

251 A commissioning experiment with a 20-mm thick target was performed
252 to validate the whole system in experimental conditions. The target was
253 inserted in the FRS beam line in the S4 experimental hall at GSI. The con-
254 trol command and hydrogen tanks for the target were located on the roof
255 of the experimental area. A stable beam of ^{54}Cr at 360 MeV/u, limited
256 to 400 000 particles/spill of 10 s, was produced by the accelerator complex
257 UNILAC+SIS [?] and delivered at the hydrogen target at an energy of
258 126 MeV/u. Data were collected during 8 hours of beam time. The reaction
259 products were identified by the calorimeter LYCCA-0 [?] (first stage of
260 projectile-like residue identification for HISPEC experiments at FAIR). The
261 energy loss and residual energy of projectile-like residues were measured with
262 telescopes composed of DSSD and CsI detectors placed at 3.6 m downstream
263 of the target. Two plastic scintillators positioned upstream and downstream
264 the target (separated by 4 m) were used to measure the time of flight of the
265 residues. 12 RISING triple clusters [?], each composed of seven Ge crystal,
266 were positioned at forward angles in close configuration (700 mm from the
267 target). A shielding composed of layers of lead and tin were placed in front
268 of each cluster to reduce the low energy background in the gamma spectra.

269 The reactions products were clearly identified in atomic number by the
270 standard ΔE -E method. The absolute mass determination was performed
271 via the measurement of the kinetic energy of each projectile and his velocity
272 after the target. A mas resolution of $\Delta A/A=1$ was achieved during this test
273 experiment.

274 On Fig.?? are shown the energy distributions obtained for residues from the

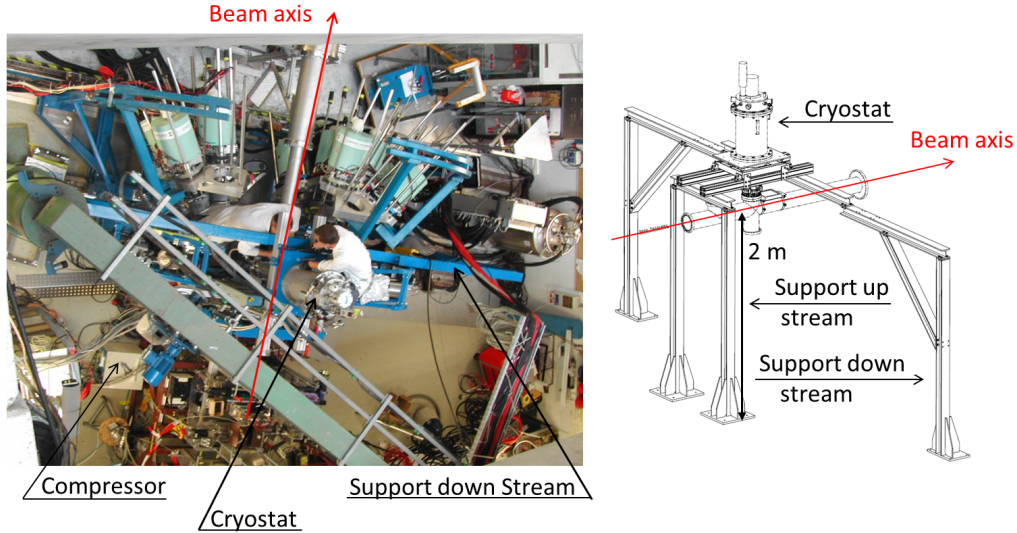


Figure 6: Top view of the experimental vault during the installation of the cryostat at the vertical of the target location. On this picture, the beam direction goes from top to bottom.

275 reactions of inelastic scattering (*a*), knockout $-1n$ (*b*), $-2n$ (*c*) and $-4n-2p$ (*d*).
 276 These distributions are obtained after a selection on the Ge time; only the
 277 edge of the peak in the Ge time distribution has been considered to overcome
 278 the γ rays coming from interactions of the beam with detectors placed either
 279 downstream or upstream the target. The γ rays detected by the crystals
 280 close to the beam line ($\theta_\gamma \leq 18^\circ$) have been excluded from the analysis, as for
 281 those crystals, the signal over background is small. The addback procedure
 282 has been done in those spectra, with no specific requirement on the gamma
 283 energy. We found that this correction improves the signal over background
 284 only for high energy transition ($E_\gamma \geq 1400$ keV). We obtained an energy
 285 resolution of 30 keV at 834 keV, close to the expected one of 26 keV calcu-
 286 lated with GEANT4 simulations. In those spectra, signal over background
 287 is around 2, but reaches 3 at 1436 keV in ^{52}Cr .

288
 289 We extracted exclusive cross sections for the population of ^{54}Cr (2^+ state),
 290 ^{53}Cr ($5/2^-$, $7/2^-$ states), ^{52}Cr (2^+ , 4^+ states), and ^{48}Ti (2^+ , 4^+ states).
 291 The corresponding Doppler-corrected gamma spectra are shown in Fig. ??.
 292 The efficiencies have been given by GEANT4 simulations. The results are

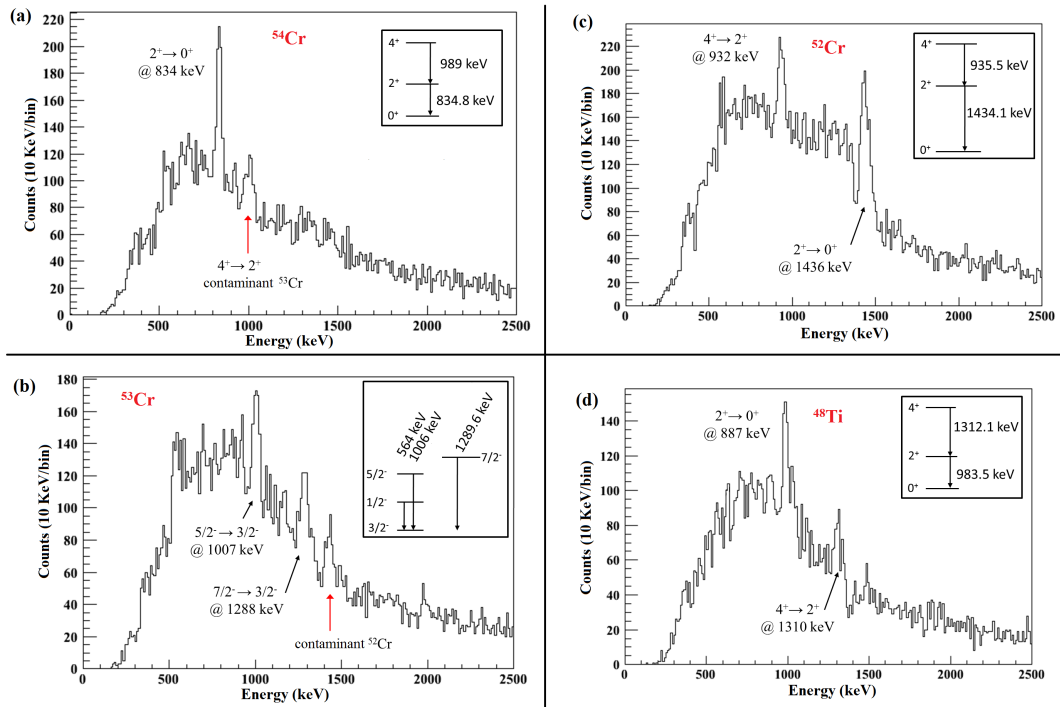


Figure 7: Gamma energy spectra in coincidence with (a) ^{54}Cr , (b) ^{53}Cr , (c) ^{52}Cr and (d) ^{48}Ti .

293 gathered in Table.???. Some theoretical predictions are also given in the table
 294 for comparison.

Table 1: Exclusive cross sections for $^{54,53,52}\text{Cr}$ and ^{48}Ti

i	σ_{exp}^i	σ_{theo}^i
2^+ of ^{54}Cr	.. mb	.. mb
$5/2^-$ of ^{53}Cr	.. mb	.. mb
$7/2^-$ of ^{53}Cr	.. mb	.. mb
2^+ of ^{52}Cr	.. mb	.. mb
4^+ of ^{52}Cr	.. mb	.. mb
2^+ of ^{48}Ti	.. mb	-
4^+ of ^{48}Ti	.. mb	-

295

296 6. Conclusion

297 A new liquid hydrogen target for in-beam gamma spectroscopy experi-
 298 ments with radioactive beams at GSI/FAIR has been built. The device is
 299 dedicated to proton-induced inclusive reactions at intermediate energies. The
 300 target is composed of a Mylar cell (typically 200 μm thick) with an effective
 301 diameter of 65 mm. The target thickness can be chosen from 10 to 80 mm.
 302 Today, two target cells have been conceived: 20-mm and 60-mm thick. The
 303 present target requires 12 hours to be conditioned from room temperature
 304 to operation mode. It can be emptied and refilled in few minutes for back-
 305 ground measurements during the data taking. A commissioning experiment
 306 was performed by use of a ^{54}Cr beam at 126 MeV/nucleon. The data taking
 307 and the data analysis showed a proper operation of the full system.

308 The target is ready for in-beamm gamma experiments with the AGATA
 309 detector at GSI and, in the future, FAIR to explore the collectivity and
 310 single-particle shell structure through inelastic scattering and knockout, re-
 311 spectively.

312 [1] H.J. Wollersheim *et al.*, Nucl. Instr. Meth. A **537**, 637-657 (2005).

313 [2] P. Dolegiewiez *et al.*, Nucl. Instr. Meth. A , (2006).

314 [3]

- 315 [4] A. Obertelli and T. Uesaka, Eur. Phys. J. A **47** 105 (2011).
- 316 [5] S. Akkoyun *et al.*, Nucl. Instr. Meth. A **668**, 26 (2011).
- 317 [6]
- 318 [7] A. Gillibert *et al.*, Eur. Phys. Jour. A (2012).
- 319 [8] H. Geissel *et al.*, NIM B 70 (1992) 286
- 320 [9] D. Rudolph *et al.*, "LYCCA technical Design Report"
- 321 <http://wwwnsg.nuclear.lu.se/lycca>